Vector Phase Conjugation and Beam Combining by Multiwave Optical Mixing

Robert W. Boyd, Kenneth R. MacDonald, and Michelle S. Malcuit

Institute of Optics

University of Rochester

Rochester, New York 14627

Introduction

This paper presents a review of the various techniques for achieving vector phase conjugation and some results on a new method for laser beam combining based on multiwave optical mixing in atomic vapors.

Vector Phase Conjugation

Let us begin by reviewing the distinction between scalar phase conjugation and vector phase conjugation (VPC). If the field $\vec{E} e^{-i\omega t} + cc$ falls onto an ideal phase-conjugate mirror (PCM), the field leaving the mirror is proportional to $\vec{E}^* e^{-i\omega t} + cc$. In order to determine the significance of replacing $\vec{E}$ by its complex conjugate, let us represent $\vec{E}$ as the product $\vec{E} = \vec{\varepsilon} A_o \exp(i\vec{k} \cdot \vec{r})$ of a complex polarization unit vector $\vec{\varepsilon}$, a slowly varying field amplitude A_o, and an exponential phase factor $\exp(i\vec{k} \cdot \vec{r})$. We then see by taking the complex conjugate of $\vec{E}$ that the action of an ideal PCM is three-fold:

$A_o \to A_o^*$, implying reversal of the wavefront;

$\vec{k} \to -\vec{k}$, implying inversion of the wavevector; and

$\vec{\varepsilon} \to \vec{\varepsilon}^*$, implying polarization conjugation.

This latter property implies, for example, that right-hand circular light remains right-hand circular in reflection from a PCM instead of becoming left-hand circular as in the case of reflection from an ordinary mirror. It is crucial to note that many devices which are known as PCMs do not possess this desirable third property. These latter devices we shall refer to as scalar PCMs and to devices that possess all three properties as vector phase-conjugate mirrors (VPCMs).

Let us consider the example shown in Fig. 1, which illustrates the importance of the polarization characteristics of phase conjugation. We assume that light which is initially linearly polarized is passed through a stressed optical component. As a result of stress birefringence, the state of polarization of the transmitted light will be scrambled. However, if this light is reflected from a vector PCM and allowed to retraverse the stressed optical component, the effects of the stress birefringence will be removed, and the exiting beam will once again be linearly polarized.

linear polarization

scrambled polarization

pcm

What is the polarization of the output signal?
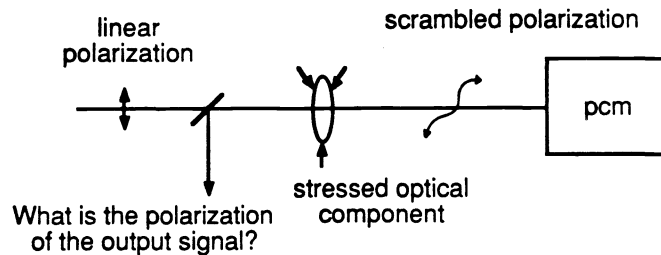
stressed optical component

Figure 1. Diagram showing schematic experimental setup to study the polarization characteristics of phase conjugation.

In order to determine the conditions under which perfect VPC will occur, it is necessary to consider the vector nature of the $\chi^{(3)}$ susceptibility used in the degenerate four-wave-mixing process leading to phase conjugation. Terhune and Maker[1] have shown that for an isotropic nonlinear material, the nonlinear polarization can always be written in the form

$$\vec{P}^{NL} = A(\vec{E}\cdot\vec{E}^*)\vec{E} + \frac{1}{2}B(\vec{E}\cdot\vec{E}^*)\vec{E}^* , \tag{1}$$

where A and B are parameters characteristic of the particular nonlinear material. Note that the second term has the vector nature of $\vec{E}^*$ and hence leads directly to VPC; on the other hand, the first term has the vector nature of $\vec{E}$ and leads to VPC only under special conditions. Vector phase conjugation would occur automatically if A were nonzero; however, for common nonlinear optical interactions A is nonzero:

B/A = 0 for electrostriction

B/A = 1 for nonresonant electronic nonlinearities

B/A = 6 for the orientational Kerr effect.

In fact, A does vanish for certain two-photon-allowed transitions, a point we will come back to later. However, since for most materials A is nonzero, special care must usually be taken to achieve VPC.

Let us now summarize some of the interactions that result in VPC.[2-11] Zel'dovich and Shkunov[2] have proposed, and Blashchuh et al.[3] have verified experimentally, that VPC is obtained if the pump waves are chosen to be linearly polarized, and the signal waves propagate along the polarization direction of the pump waves. As one can see by inspection of Eq. (1), in this case the term proportional to A does not contribute to the nonlinear polarization and hence only the second term, which always leads to VPC, contributes to $\vec{P}^{NL}$. However, the applicability of this technique is limited because of the poor spatial overlap between pump and signal waves.

A more generally useful configuration that leads to VPC is four-wave mixing with circularly polarized, counter-rotating pump beams. To see why this interaction leads to VPC, we recall that the degenerate-four-wave-mixing process can be viewed as the simultaneous annihilation of one pump photon from each pump beam and the creation of a signal photon and a phase-conjugate photon. Since the two pump waves are counter-rotating, the absorption of two pump photons removes no angular momentum from the input fields. Consequently, the signal and conjugate photons must be emitted with equal and opposite angular momenta, implying that perfect polarization conjugation occurs.

We have performed an experiment to verify that we can correct for stress birefringence using VPC based on degenerate four-wave mixing with counter-rotating pump waves. A linearly polarized laser beam is passed through a stressed optical component, reflected from the PCM, and passed back through the optical component, as shown in Fig. 2. The state of polarization of the beam after it has passed back through the optical component is determined using a polarizing beam splitter and detectors. If the VPC is perfect, the output beam will be polarized in the x direction. Any imperfection in the VPC process will lead to a polarization component in the y direction.
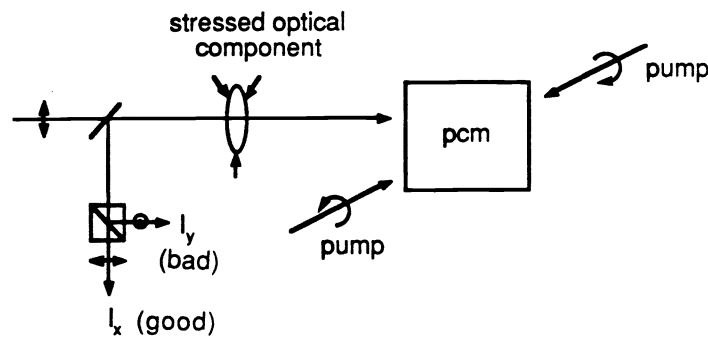

Figure 2. Experimental setup used to demonstrate polarization aberration correction by four-wave mixing using circularly polarized, counter-rotating pump beams.

Our results are shown in Figure 3. This figure shows the stressed optic as viewed between crossed polarizers and illustrates the severity of the polarization distortion. The lower figures show that VPC has corrected the polarization distortion nearly perfectly. The three spots of light in the wrong polarization result from depolarized scattering from the points of contact between the optical surface and the machine screws used to stress the component.

In order to quantify these results on the correction of polarization aberrations, we have repeated the experiment with the polarization distorter replaced by a quarter-wave plate. By varying the orientation angle θ of the waveplate, we are able to impose a known polarization aberration onto the beam. Our results are shown in Fig. 4. For the case of counter-rotating pump beams, the intensity of the "good" component is much larger than that of the "bad" component for any orientation of the waveplate and hence for any state of polarization of the light at the PCM. For comparison we have repeated the experiment using corotating pump beams. We then find that the good and bad components

stressed optic viewed between crossed polarizers

corrected image
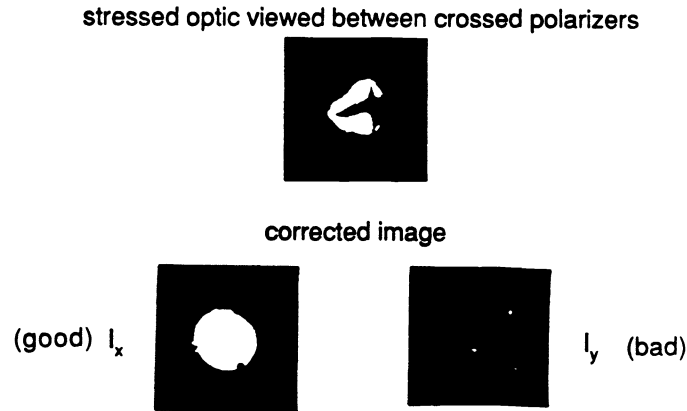
(good) I_x

I_y (bad)

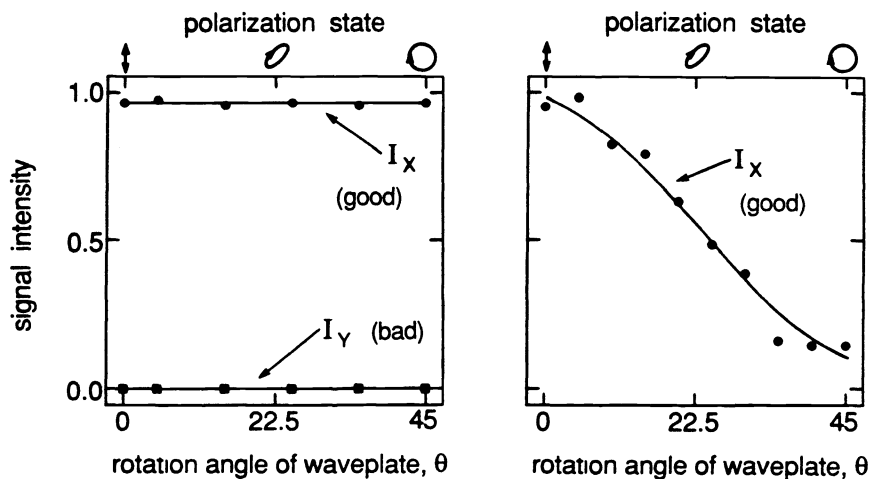Figure 3. Photographs demonstrating polarization-aberration correction by VPC.

Figure 4. Intensities of each polarization component plotted as a function of the degree of polarization distortion introduced into the probe wave. (a) For circularly polarized, counter-rotating pump beams, the effects of the polarization distortion are removed essentially completely ($I_x >> I_y$ and I_x is independent of θ) (b) For circularly polarized, corotating pump beams, the quality of VPC is severely degraded (I_x and I_y are comparable and depend on θ).

are comparable in magnitude and vary with the state of polarization, demonstrating that this configuration does not correct for polarization aberrations.

There are certain types of aberration that cannot be corrected even by VPC. For example, VPC cannot correct for distortion resulting from the Faraday effect. As shown in Fig. 5, a linearly polarized laser beam was passed through a Faraday rotator, which rotated the beam's polarization by an angle β. Rather than being removed by the VPC process, the total rotation angle is doubled after a second pass through the Faraday rotator. This is a consequence of the fact that the Faraday effect does not obey time-reversal invariance. Optical phase conjugation can be viewed as
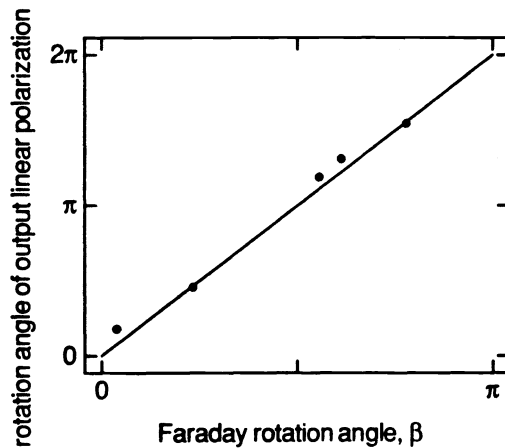
Figure 5. Rotation angle of the polarization vector of linearly polarized radiation after reflection from a vector phase conjugate mirror and retraversal through a Faraday rotator plotted as a function of the rotation angle β of the Faraday rotator.

generation of a time-reversed wavefront, and only aberrations that obey time-reversal invariance can be removed by optical phase conjugation.

The experimental results shown in Figures 3-5 could be performed using low-intensity, cw laser beams because the nonlinear-optical material we used, fluorescein-doped borate glass,[12] has a very large $\chi^{(3)}$ susceptibility. In many cases, composite materials fabricated by doping organic molecules into low-melting-temperature-glass hosts are low-intensity saturable absorbers. In the case of fluorescein-doped borate glass, the saturation intensity is 10 mW/cm^2, implying an effective third-order susceptibility of $|\chi^{(3)}| = 1$ esu. Note, for comparison, that carbon disulfide has a value of $\chi^{(3)} = 2 \times 10^{-12}$ esu. On the other hand, fluorescein-doped borate glass is quite slow: its response time is 0.1 sec versus 10^{-12} sec for carbon disulfide. There are many applications for which a large nonlinearity is more important than fast response. We consider next one such application.

As a rule, phase conjugation can remove the effects of aberrations only in double pass. We have recently devised a method[13] which in certain circumstances can be used to perform single-pass aberration correction. The idea behind this technique is illustrated in Fig. 6. Light from an extended object passes through a thin phase aberrator and forms an aberrated image of the object. If light from an object known to be a point source passes through the same aberrator, the aberrated image of the point source provides information regarding the nature of the aberrator. In order to restore the image of the extended object, we bring it into a FWM region as the probe beam. A plane pump wave and the aberrated image of the point source form the pump waves. Since the nonlinear polarization is proportional to

$$P^{NL} \sim (E_1 e^{i\Phi})(E_2)(E_3 e^{i\Phi})^* = E_1 E_2 E_3^*, \tag{2}$$

the phase distortion Φ introduced by the aberrator does not appear in the final expression for P^{NL} and the corrected image of the extended object can be recovered. In our experiment, we used a stencil of the letters *ur* as the extended object and a piece of etched glass as the aberrator. The results, also shown in Fig. 6, demonstrate that the original image is largely restored by this technique. Our long-term goal is to apply this technique to the problem of astronomical imaging. However, in order to do so, materials with values of $\chi^{(3)}$ larger than those currently available would be required.
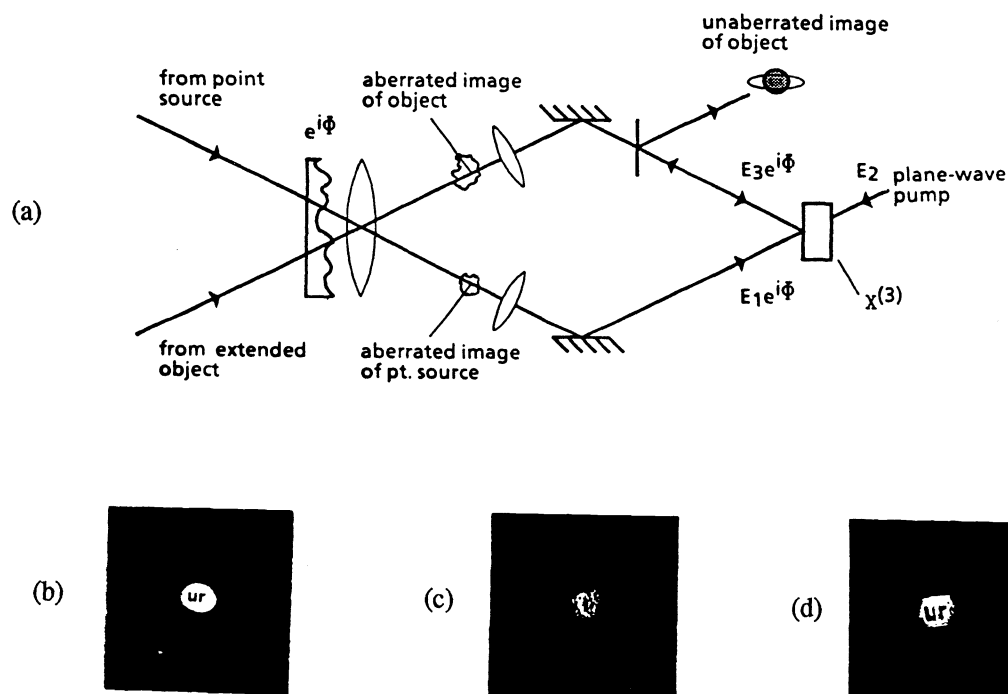

Figure 6. (a) Schematic experimental arrangement for passive, one-way phase-aberration correction using four-wave mixing. (b)-(c) Photographs demonstrating aberration correction using four-wave mixing. The input image (b) is severely aberrated (c) by a phase distorter. The restored image (d) is recovered on the other side of the aberrator from the original object.

The configurations for VPC described above require that the pump waves be in a particular state of polarization. Consequently, any imperfections in the polarizations of the pump waves will also lead to a degradation of the vector nature of the phase-conjugation process. Grynberg[10] has pointed out that if the nonlinear coupling is due to a two-photon transition between S states, as illustrated in Fig. 7, perfect VPC will occur. An intuitive explanation for this result is that, since the transition between two S states occurs with no net change in angular momentum, the signal and conjugate photons must carry equal and opposite angular momenta and hence be polarization conjugates of each other.

We have performed a density-matrix calculation which shows that to third order in the applied fields the nonlinear polarization is given by Eq. (1) with A = 0 and B given by

$$B = \frac{N|\mu_{ns \to n'p} \ \mu_{n'p \to n''s}|^2}{\hbar^3 \Delta_1^2 (\Delta_2 - i/T_2)} \tag{2}$$

so that VPC is predicted for any states of polarization of the pump waves. This prediction is so striking that it leads us to ask why the polarization characteristics of two-photon resonantly enhanced degenerate four-wave mixing are so unusual. For the two-photon case, degenerate four-wave mixing is due to scattering of the signal wave from a spatially uniform, temporally varying (at 2ω) coherence induced by the two pump waves. Conversely, for the more usual case in which the nonlinearity is due to a one-photon resonance, degenerate four-wave mixing is due to scattering of one pump wave from a temporally uniform (dc), spatially varying refractive-index distribution (grating) induced by the interference between the probe and the other pump wave.
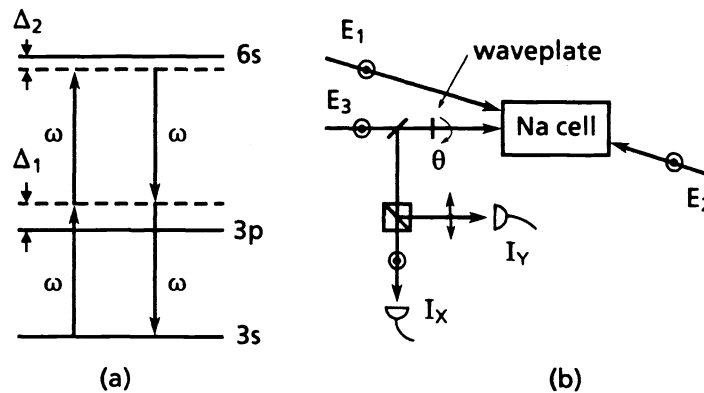

Figure 7. (a) Energy-level diagram showing the two-photon resonantly enhanced DFWM process. (b) Experimental setup used to study VPC by two-photon-resonant DFWM.

We have verified experimentally using the setup shown in Fig. 7 that two-photon resonantly enhanced degenerate four-wave mixing leads to VPC[11]. Our results are shown in Fig. 8. Note that for low pump intensity ($I/I_s = 0.1$), high quality VPC is observed. However, for the case of high pump intensity ($I/I_s = 2$), where the predictions of the third-order theory described above are not applicable, severe degradation of the fidelity of the polarization conjugation is observed.
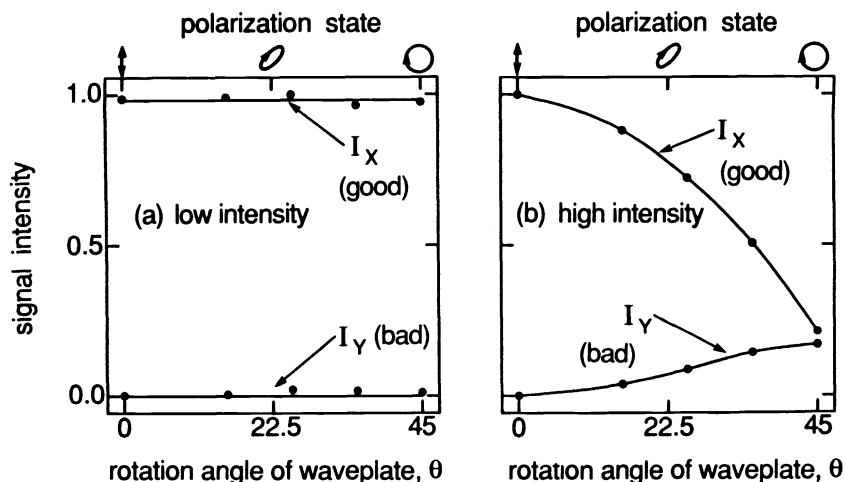
Figure 8. Intensity of each polarization component plotted as a function of the degree of polarization distortion introduced into the probe wave. (a) For low pump intensities the effects of the polarization distortion are removed essentially completely. (b) For high pump intensities, severe degradation of the VPC process is observed.

Laser Beam Combining

Laser beam combining is a process in which the interaction of two laser beams results in a single beam which contains essentially all of the energy of the two input beams, as illustrated schematically in Fig. 9. Of course, more than two beams can be combined by cascading a number of such devices. We have performed a set of experiments using two tunable dye lasers and atomic sodium vapor which shows that it is possible to amplify a weak probe beam due to its interaction in an atomic vapor with a strong pump beam.[14] A 38-fold increase in the probe intensity was achieved in this study using only a 7 mm path length of sodium vapor. A second experiment, still in progress, is aimed at combining two equal-intensity, pulsed alexandrite laser beams in atomic potassium vapor.
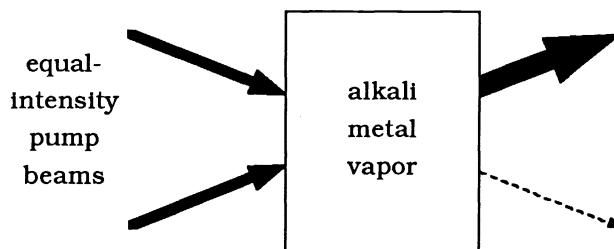

Figure 9. Nonlinear interactions can be utilized to coherently combine two input beams into a single output beam which contains nearly all of the incident power.

The interaction between a two-level atomic system and an intense, nearly resonant laser field (Fig. 10a) modifies the atomic energy level structure as a consequence of the AC Stark effect.[15] The Rabi cycling of population between the upper and lower atomic levels effectively splits each level into a doublet with a separation equal to the generalized Rabi frequency

$$\Omega' = \operatorname{sgn}(\Delta) \, (\Omega^2 + \Delta^2)^{1/2} \tag{3}$$

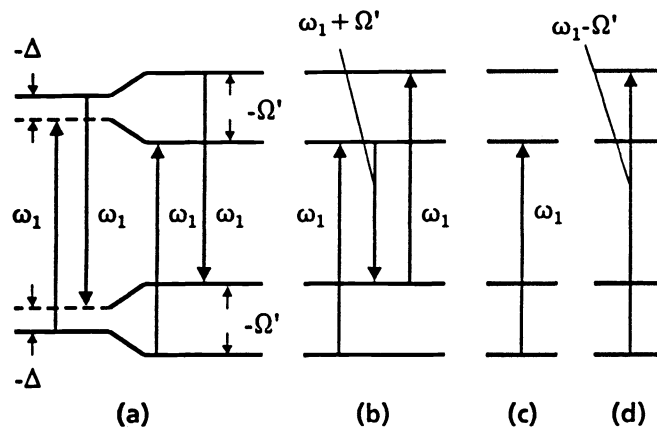where $\Omega = |\mu_{ba}| E_1 / \hbar$. The modified atomic states are known as "dressed states."[16]

Figure 10. (a) In the presence of a strong, nearly resonant optical field, the ground and excited states of an atom are split into doublets separated by the generalized Rabi frequency Ω'. The transitions (b-d) between the modified levels correspond to the resonances in the absorption spectrum shown in Fig. 11.

As a result of the shifting and splitting of the atomic levels, the absorption spectrum measured by a weak probe wave has the form shown in Fig. 11. The spectrum is composed of three distinct resonances, two of which can become negative, implying amplification of the probe wave. The first feature (b), detuned from the laser by the generalized Rabi frequency, gives rise to amplification by means of the stimulated 3-photon effect, in which the atom makes a transition from the lowest to the highest dressed state by the simultaneous absorption of two pump photons and the emission of a Rabi sideband photon (Fig. 10b). The second feature (c), which is centered on the pump laser frequency, results from the interaction of the atomic population with the intensity beat between the pump and probe laser beams (Fig. 11b).[17] The large positive-going (ie, lossy) feature (d) is the shifted atomic resonance and corresponds to a transition from the lowest dressed state to the highest dressed state (Fig 10d). These spectral features have been observed by Wu et al.[18] in an atomic beam experiment. The goal of our work was to see if these effects persist in an atomic vapor, where much higher atomic number densities, and hence larger nonlinearities, can be obtained.

Typical experimental results are shown in Fig. 12. In this experiment the atomic number density was 3×10^{13} atoms/cm^3, the pump laser intensity was 300 W/cm^2, the background pressure of helium buffer gas was 4 torr, and the crossing angle between the beams was 1.6 degrees. The pump laser is tuned $\sim$2GHz to the low frequency side of the D_2 sodium resonance line. In the particular case illustrated, amplification at the Rabi sideband leads to an approximately eight-fold increase in the probe laser intensity. Note that a smaller but still significant amount of gain is present at the central feature. For comparison, a theoretical plot which assumes the value $T_2/T_1 = 0.28$ (where T_2 and T_1 are the coherence and population lifetimes, respectively). There is good agreement betweeen the theoretical and experimental spectra. The arrows below the x-axes denote the approximate resonant frequencies for transitions from the hyperfine-split levels in the ground state of sodium, and the resonance frequency of the two-level system assumed in the theoretical model, respectively.
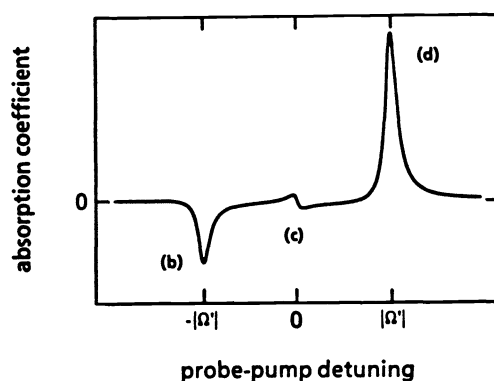

Figure 11. The modification of a two-level atomic system by a strong laser field gives rise to a probe absorption spectrum with three resonance features.
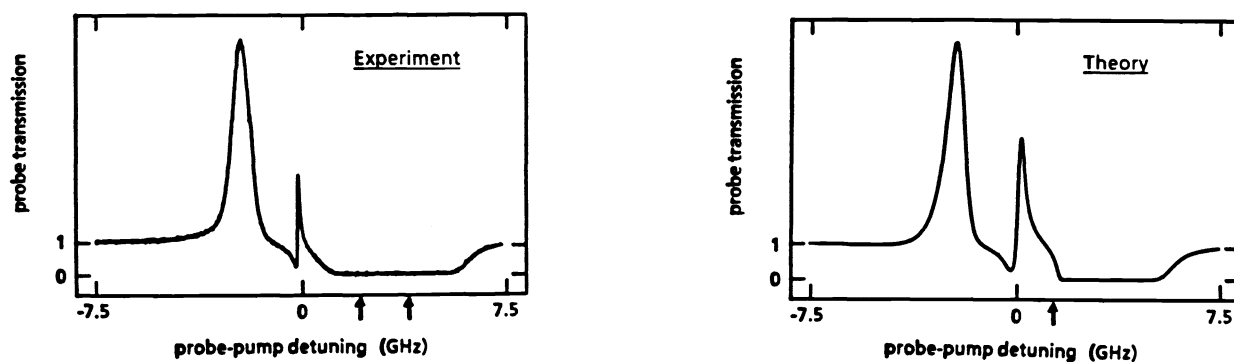

Figure 12. The experimentally measured probe transmission spectrum (left) is compared to the corresponding theoretical transmission spectrum (right).

In conclusion, we have seen how VPC can be implemented and used to remove the effects of polarization distortions from optical systems. We have also presented new results on laser beam combining by multiwave optical mixing in atomic vapors.

Acknowledgements

References

1. P. D. Maker and R. W. Terhune, Phys. Rev. **137**, A801 (1965).

2. B. Ya. Zel' dovich and V. V. Shkunov, Sov. J. Quantum Electron. **9**, 379 (1979).

3. V. N. Blaschuk, B. Ya. Zel' dovich, A. V. Mamaev, N. F. Pilipetsky, and V. V. Shkunov, Sov. J. Quantum Electron. **10**, 356 (1980).

4. G. Martin, L. L. Lam, and R. W. Hellwarth, Opt. Lett. **5**, 185 (1980).

5. N. G. Basov, V. F. Efimkov, I. G. Zuberev, A. V. Kotov, S. I. Mikhailov, and M. G. Smirnov, JETP Lett. **28**, 197 (1978).

6. I. McMichael, M. Khoshnevisan, and P. Yeh, Opt. Lett. **11**, 525 (1986).

7. I. McMichael, P. Yeh, and P. Beckwith, Opt. Lett. **12**, 507 (1987).

8. I. McMichael, J. Opt. Soc. Am. B **5**, 863 (1988).

9. K. Kyuma, A. Yariv, and S.-K. Kwong, Appl. Phys. Lett. **49**, 617 (1986).

10. G. Grynberg, Opt. Commun. **48**, 432 (1984).

11. M. S. Malcuit, D. J. Gauthier, and R. W. Boyd, Opt. Lett. **13**, 663 (1988).

12. M. A. Kramer, W. R. Tompkin, and R. W. Boyd, Phys. Rev. A **34**, 2026 (1986).

13. K. R. MacDonald, W. R. Tompkin, and R. W. Boyd, Opt. Lett. **13**, 485 (1988).

14. M. T. Gruneisen, K. R. MacDonald, and R. W. Boyd, J. Opt. Soc. Am. B **5**, 123 (1988).

15. B. R. Mollow, Phys. Rev. **188**, 1969 (1969); F. Schuda, C. R. Stroud, Jr., and M. Hercher, J. Phys. B **7**, L198 (1974).

16. C. Cohen-Tannoudji and S. Reynaud, J. Phys. B **10**, 345 (1977); **10**, 365 (1977); **10**, 2311 (1977); E. Courtens and A. Szöke, Phys. Rev. A **15**, 1588 (1977); errata, **17**, 2119 (1978).

17. R. W. Boyd, M. G. Raymer, P. Narum, and D. J. Harter, Phys. Rev. A **24**, 411 (1981); M. Sargent III, Phys. Rep. **43**, 223 (1978); S. E. Schwartz and T. Y. Tan, Appl. Phys. Lett. **10**, 4 (1967); L. W. Hillman, R. W. Boyd, J. Krasinski, and C. R. Stroud, Jr., Opt. Comm. **45**, 416 (1983); M. S. Malcuit, R. W. Boyd, L. W. Hillman, J. Krasinski, and C. R. Stroud, Jr., J. Opt. Soc. Am. B **1**, 73 (1984).

18. F. Y. Wu, S. Ezekiel, M. Ducloy, and B. R. Mollow, Phys. Rev. Lett. **38**, 1077 (1977).